



GAS TURBULENCE MODULATION IN THE PNEUMATIC CONVEYING OF MASSIVE PARTICLES IN VERTICAL TUBES

EDUARDO J. BOLIO and JENNIFER L. SINCLAIR†

Department of Chemical Engineering, Carnegie Mellon University, Pittsburgh, PA 15213, U.S.A.

(Received 15 June 1994; in revised form 5 January 1995)

Abstract—The present work is concerned with the interaction between large particles and gas phase turbulence. Gas turbulence modulation in these systems is considered to be dominated by a generation mechanism which arises due to the presence of wakes behind particles. Following a recent proposal, a closure for gas turbulence modulation accounting for the effect of wakes is employed within the context of a mathematical model for particle-laden, turbulent flows. The model accounts for particle–particle and particle–wall interactions associated with larger particles based on concepts from gas kinetic theory. It is shown that due to the significant flattening of the mean gas velocity profile with the addition of particles, and the corresponding decrease in turbulent energy production, a generation mechanism must be present in order to produce gas velocity fluctuation predictions which are consistent with the experimental measurements, even in the case where the experimental results indicate a net suppression of gas phase turbulence in the presence of particles.

Key Words: two-phase flow, turbulence, pneumatic transport, particle–particle interactions, particle–turbulence interactions

INTRODUCTION

The dynamics of gas–solid flows are important in many engineering equipment and processes. A few examples include pneumatic conveying, cyclone separators, circulating fluidized beds and entrained-flow gasifiers. A key step towards understanding the complex flow behavior of these systems is to understand the interaction between particles and the turbulent structure of the carrier fluid. Recent efforts which have focused on the hydrodynamic modeling of gas–solids flow in the case of larger particles treat the particle phase as a rapid granular flow and employ concepts from the kinetic theory of dense gases to describe the momentum and kinetic energy transferred by the velocity fluctuations of the particles (Sinclair & Jackson 1989; Ding & Gidaspow 1990; Pita & Sundaresan 1993; Ocone *et al.* 1993). These efforts, in general, have neglected gas phase turbulence and the effect of particles on modulating gas turbulent intensity. Two notable exceptions are the works of Louge *et al.* (1991) and Bolio *et al.* (1995). In these two models, turbulence in the gas phase is described by employing the eddy viscosity concept, and the eddy viscosity is given by the solution of one transport equation and two transport equations, respectively, which are modified for the presence of a dilute particle phase.

In the work of Bolio *et al.* (1995), it was shown that the significant flow features observed in the experimental data for dilute gas–solid flow in the case of larger particles are predicted. The model is able to predict a decrease in the relative velocity with increasing solid loading m (ratio of solids mass flux to gas mass flux) and decreasing particle size, as well as the flattening of the mean gas velocity profile with the addition of solids. The particle velocity fluctuations are generated by particle–particle and particle–wall interactions, and the particle fluctuation intensity can exceed the gas fluctuation intensity. Perhaps most significant were the comparisons of model predictions for the particle velocity fluctuations with the experimental data of Tsuji (1993). These comparisons revealed that the type of treatment which includes particle–particle interactions associated with larger particles is highly successful in predicting the particle fluctuation velocity of a dilute concentration of particles (particle diameter $d = 200 \mu\text{m}$) in a gas stream. It was also shown that inelastic particle–particle collisions can give rise to the large relative velocities, several times greater

†To whom correspondence should be addressed.

than the particle terminal velocity. The predicted solid velocity profiles were flatter than the corresponding gas velocity profiles, and, hence, the relative velocity changed signs near the pipe wall, at approximately $r/R = 0.9$, consistent with experimental data.

The one flow variable that was not adequately captured in the previous model of Bolio *et al.* (1995) was the turbulent kinetic energy of the gas phase since the description for the rate of gas kinetic energy change per unit volume was dominated by a dissipative mechanism where particles extract energy from the flow due to a drag effect. Hence, for all of the operating conditions that were considered, the predicted turbulent intensity of the gas was significantly lower than the experimental measurements. However, for larger particles that do not follow the fluid motion, one might instead expect that a generation mechanism such as one due to the presence of wakes trailing each particle or vortex shedding would contribute to the gas velocity disturbance and would be the dominating factor in gas turbulence modulation. Also, in the case of large particles, where the particle relaxation time is very large relative to the particle–eddy interaction time, the particle velocity does not change appreciably during the time of interaction and the contribution of turbulence reduction to the total turbulence modulation should be small (Yuan & Michaelides 1992).

It is the aim of this present work to build on the previous model of Bolio *et al.* (1995) to include a more appropriate description of gas turbulence modulation in the presence of larger particles. The framework of the previous modeling effort will be retained; that is, the model includes inelastic particle–particle interactions described by kinetic theory analogies, and boundary conditions for the solid phase are based on collisional exchanges of tangential momentum and energy at the wall. This present model, however, includes a theoretical description for turbulence generation taking into account the turbulent wakes behind larger particles following a recent proposal by Yuan & Michaelides (1992).

GOVERNING EQUATIONS

We analyze the case of steady, fully-developed turbulent flow of a gas–solid mixture in a vertical pipe. The particle phase is regarded as a continuum and the corresponding balance of momentum for the particle phase can be obtained by local averaging of the equation of motion for the center of mass of a single particle through regions large enough to contain many particles but small with respect to the bounding container. The averaging procedure leads to terms which describe the variety of interactions associated with the velocity fields of the two phases. Accurate hydrodynamic predictions rest on correct descriptions for these various interactions.

For the case outline above, the vertical z -component of the momentum equation for the gas phase becomes

$$0 = -\frac{\partial p}{\partial z} - \beta(v_z - u_z) + \frac{1}{r} \frac{\partial}{\partial r} (r\tau_{rz}^I) \quad [1]$$

with

$$\tau_{rz}^I = \mu \frac{\partial v_z}{\partial r} - \overline{\rho v_r' v_z'} \quad [2]$$

In these equations, v and u represent the mean gas and solid velocities, v' and u' represent the fluctuating gas and solid velocities, p is the gas phase pressure and μ is the intrinsic gas viscosity. The form for drag coefficient β is adopted from the expression used by Ding & Gidaspow (1990). It is assumed that the eddy viscosity μ_t is uniquely determined by the turbulent kinetic energy k and its dissipation rate ϵ via the Kolmogorov–Prandtl relation

$$\mu_t = \frac{f_\mu \rho_G k^2}{\epsilon} \quad [3]$$

where ρ_G is the gas density and f_μ is a function of the turbulent Reynolds number Re_τ and the dimensionless distance from the wall y^+ .

For two-phase flow, the particle phase turbulent kinetic energy equation and its dissipation rate equation must be modified to include the presence of the particles.

$$0 = \frac{1}{r} \frac{\partial}{\partial r} \left\{ r(1-v) \left(\mu + \frac{\mu_t}{\sigma_k} \right) \frac{\partial k}{\partial r} \right\} + (1-v) \mu_t \left(\frac{\partial v_z}{\partial r} \right)^2 - \rho_G \epsilon (1-v) + \Delta K \quad [4]$$

$$0 = \frac{1}{r} \frac{\partial}{\partial r} \left\{ r(1-v) \left(\mu + \frac{\mu_t}{\sigma_c} \right) \frac{\partial c}{\partial r} \right\} + f_1 \frac{c}{k} (1-v) \mu_t \left(\frac{\partial v_z}{\partial r} \right)^2 - f_2 \rho_G (1-v) \frac{c^2}{k} - c_3 \Delta K \frac{c}{k} \quad [5]$$

The last term in the turbulent kinetic energy equation accounts for the influence of the particles on the turbulent fluctuations in the gas, which can either dampen or enhance these fluctuations, where ΔK is the rate of kinetic energy change per unit volume.

In the hydrodynamic models of Louge *et al.* (1991) and Bolio *et al.* (1995) this term was given as

$$\Delta K = -\beta(1-v) \overline{v'_i(v'_i - u'_i)} = -\beta(1-v)(2k - \overline{v'_i u'_i}) \quad [6]$$

where the correlation $\overline{v'_i u'_i}$ is modeled, as a tentative first attempt, by extending a theoretical treatment by Koch (1990) who considered the case of a dilute gas–solid suspension at low particle Reynolds number in the limit where the particle velocity distribution function was controlled by solid–body interactions.

$$\overline{v'_i u'_i} = \frac{4}{\sqrt{\pi}} \frac{d}{\rho_s} \beta \frac{(1-v)}{v} \frac{(v_z - u_z)^2}{\sqrt{T}} \quad [7]$$

Here T is a “particle temperature” which is a measure of the magnitude of the particle velocity fluctuations [$T = \frac{1}{3} \overline{(u'_i)^2}$]. As discussed in the introduction, the previous description for gas turbulence modulation [6] was dominated by the dissipative portion, and the resulting model predictions for the gas velocity fluctuations were significantly lower than the experimental measurements indicated.

Hence, in this paper we investigate a theoretical description for gas turbulence modulation (ΔK) which involves enhancement of gas phase velocity fluctuations in the presence of larger particles due to the presence of wakes behind the particles, as recently proposed by Yuan & Michaelides (1992). In the treatment of Yuan & Michaelides, the change in the kinetic energy associated with turbulent production is proportional to the difference of the squares of the two velocities and to the wake volume W_v , where the velocity disturbance occurs.

$$\Delta k = \frac{1}{2} \rho_G W_v (v_z^2 - u_z^2) \quad [8]$$

Yuan & Michaelides assume that the wake shape is half of a complete ellipsoid with a base diameter d and a height equal to the wake length W_1 . Therefore the wake volume is given as

$$W_v = \frac{\pi d^2 W_1}{6} \quad [9]$$

An improved estimate of the wake shape is depicted in figure 1. The wake shape is approximated by the region between an ellipsoidal body and the spherical particle. By geometrical considerations,

$$W_v = \frac{\pi(W_1 + h)d^2 \sin^2 \Theta}{6} - \frac{\pi h^2}{3} \left(\frac{3d}{2} - h \right) \quad [10]$$

$$h = \frac{d}{2} (1 - \cos \Theta) \quad [11]$$

For dilute flow, the wake length W_1 and the separation angle Θ are functions of the particle Reynolds number Re_p and are given by correlations developed for flow past a sphere. When the separation angle Θ is 90° , the improved estimate for the wake volume W_v ([10] and [11]) equals that originally proposed by Yuan & Michaelides (1992) ([9]). In this study, the wake length and separation angle are obtained from the work of Rimón & Cheng (1969) who found the wake onset at a Re_p approximately equal to 10.

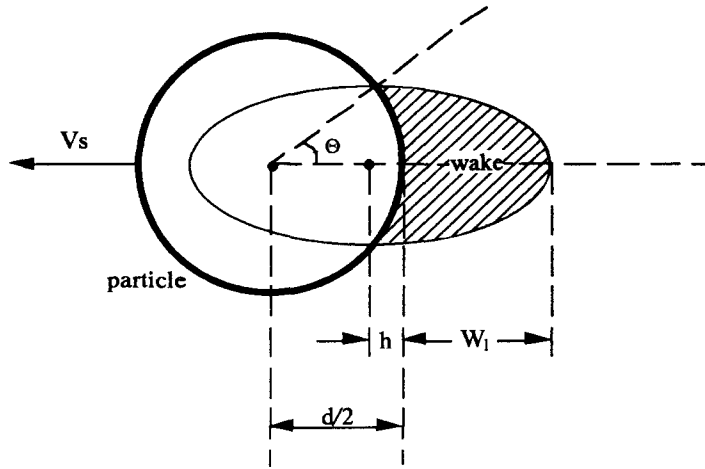


Figure 1. Representation of a wake trailing a particle.

The rate of kinetic energy change per unit volume is expressed as the product of the kinetic energy gain per particle–eddy interaction, the interaction frequency and the number of particles per unit volume

$$\Delta K = [\Delta k] \left[\frac{6v}{\pi d^3} \right] [t_i^{-1}] \tag{12}$$

where the eddy–particle interaction time t_i is the minimum of the eddy lifetime or the time it takes a particle to cross an eddy

$$t_i = \min \left(\frac{l_e}{(v_z - u_z)}, \frac{\rho_G l_e^2}{\mu_t} \right) \tag{13}$$

and the characteristic eddy length l_e is given as

$$l_e = \left(\frac{\mu_t^3}{\epsilon \rho_G^3} \right)^{1/4} \tag{14}$$

In the results which we will present, the time to cross an eddy is the minimum of the two time scales over most of the tube cross-section, except near the radial location corresponding to the crossover of the mean gas and particle velocity fields.

The base ($v = 0$) $k-\epsilon$ closure model used is the low-Reynolds number Myong & Kasagi (1990) model. The turbulence model was validated for pure gas by comparing the model predictions with the experimental data for the mean and fluctuating gas velocity of Schildknecht *et al.* (1979) over a range of Reynolds numbers (Hrenya *et al.* 1995). The predicted profiles for the mean gas velocity and turbulent intensity were in exact agreement with the measured profiles. As a first approximation, the $k-\epsilon$ constants and functions associated with this single-phase model are retained in this work with $c_3 = 1.2$. Since the use of these same values is speculative for dilute two-phase flow, a thorough sensitivity analysis was performed in Bolio *et al.* (1995), exploring the extent to which the results depend on this choice of values. The influence on the mean and fluctuating velocity profiles and the solid concentration profiles was seen to be small, and in some cases imperceptible.

For the particle phase, the particles are assumed to be cohesionless and uniform in size, and the z - and r -components of the momentum equations are

$$0 = -\frac{1}{r} \frac{\partial}{\partial r} (r\sigma_{rz}) + \beta(v_z - u_z) - \rho_s v g \tag{15}$$

$$0 = \frac{1}{r} \frac{\partial}{\partial r} (r\sigma_{rr}) - \frac{\sigma_{\theta\theta}}{r} \tag{16}$$

Stresses within the particle assembly and the effective viscosity and pressure of the particle phase depend strongly on the particle temperature; thus, this must be found by solution of a separate

differential equation representing a balance for the kinetic energy associated with the individual particle velocity fluctuations, or the “granular energy”.

$$0 = -\frac{\partial q_{PT}}{\partial r} - \frac{q_{PT}}{r} - \sigma_{rz} \frac{\partial u_z}{\partial r} - \gamma + \beta(1 - \nu) \overline{u'_i(v'_i - u'_i)} \quad [17]$$

Granular energy is conducted as a result of gradients in the particle temperature (analogous to heat conduction due to gradients in the thermodynamic temperature), generated by the working of the effective shear stresses in the particle phase (third term), dissipated by the inelasticity of collisions between particles (fourth term). The last term represents a source or sink of granular energy due to the gas–particle interactions. In this term the sink contribution dominates, as discussed in Ding & Gidaspow (1990). In order to close these equations, the constitutive relations of Lun *et al.* (1984), with a few modifications, are used for the particle phase stress tensor σ , the granular energy flux vector \mathbf{q} , and the dissipation rate of granular energy γ due to inelastic particle–particle collisions (Sinclair & Jackson 1989).

In summary, the particle-laden turbulent flow model consists of six coupled differential equations [1], [4], [5], [15], [16] and [17] which describe the relationship between the mean and fluctuating components of the gas and solid velocities and the pressure gradient. The complete formulation of the model requires boundary conditions at the tube wall and centerline. At the axis of the pipe, symmetry clearly demands that the gradients of all the variables be zero. At the wall, boundary conditions are needed for the particle velocity and the particle temperature. In general it is not permissible to set the particle velocity and the particle temperature equal to zero at a solid wall. Exceptions occur when the wall is sufficiently rough, minimizing particle slip, and when the bounding wall is sufficiently “soft”, creating highly inelastic particle–wall collisions. A boundary condition for the particle velocity is found by equating the limit of the shear stress in the particle phase, on approaching the wall, to the transfer rate of momentum to the wall by particles that collide with it (Johnson & Jackson 1987):

$$\sigma_{rz} = \frac{\rho_s \pi u_z \phi \sqrt{T}}{2\sqrt{3} \left(\frac{v_o}{v} - \frac{v_o^{2/3}}{v^{2/3}} \right)} \quad [18]$$

The specularity factor ϕ represents the fraction of momentum transferred to the wall when particles collide with it. A boundary condition for the particle temperature at the wall is obtained from an energy balance on a thin region adjacent to the solid surface (Johnson & Jackson 1987):

$$q_r + \frac{\rho_s \pi u_z^2 \phi \sqrt{T}}{2\sqrt{3} \left(\frac{v_o}{v} - \frac{v_o^{2/3}}{v^{2/3}} \right)} - \frac{\sqrt{3} \rho_s \pi (1 - e_w^2) T^{3/2}}{4 \left(\frac{v_o}{v} - \frac{v_o^{2/3}}{v^{2/3}} \right)} = 0 \quad [19]$$

Physically, the second term represents an increase in particle temperature due to particle slip at the wall. The last term represents a decrease of particle temperature when particles collide inelastically with the wall. For elastic particle–wall collisions, the coefficient of restitution for particle–wall collisions e_w equals one, and this term is zero.

EXPERIMENTAL DATA

To the authors’ knowledge there are only three LDV data sets for vertical gas–solids flow in a pipe (Maeda *et al.* 1980; Lee & Durst 1982; Tsuji *et al.* 1984). All of these data are for solid loading ratios less than five. In this paper we focus on the data by Tsuji *et al.* (1984) since it is the most comprehensive. Tsuji *et al.* consider different particle sizes and vary the solid loading ratio for each size. Experimental data are given for the mean gas and particle velocity profiles, as well as the r.m.s. axial gas velocity fluctuations. Unfortunately, the conditions at which the mean velocity data are reported are different than the conditions at which the fluctuating velocity data are given. Recently, Tsuji (1993) has revisited his previous data and has extracted the r.m.s. axial solid velocity fluctuations. These data are given in Bolio *et al.* (1995).

For the fluctuating velocity data, it should also be re-emphasized that only the axial fluctuating velocity component has been reported in all of data sets mentioned above. Hence, perfect agreement

between model predictions employing a $k-\epsilon$ closure scheme and experimental data should not be expected at the level of the axial fluctuating velocity component, particularly in the near-wall region, where the anisotropic effects in the flow are more important. In figure 2 we show a validation of the base turbulence model; that is, the system of equations is first solved for the case of clear gas and compared with the single phase experimental data of Tsuji *et al.* (1984). This type of discrepancy at the level of one fluctuating component is similar to what we have shown in Bolio *et al.* (1995) when we compared the single phase model predictions at two levels, the total turbulent kinetic energy (in which model predictions exhibit perfect agreement with the data) and the axial fluctuating component (in which model predictions fall below the data near the wall), with the experimental data of Schildknecht *et al.* (1979). Although more sophisticated turbulent closure models which account for the anisotropic nature of turbulence are available, studies by Martinuzzi & Pollard (1989) indicate that the predictions from a low-Reynolds $k-\epsilon$ closure scheme are in better agreement with pipe flow data.

In figure 3(a) and (b) we have reproduced the gas fluctuating velocity data of Tsuji *et al.* (1984) for the 200 and 500 μm polystyrene spheres ($\rho_s = 1020 \text{ kg/m}^3$) in order to discuss qualitatively the trends observed in the modulation of gas phase turbulence due to the addition of particles. For the 200 μm spheres, the turbulent kinetic energy for the two-phase flow is less than the clear gas intensity throughout the pipe section. An analysis of the turbulent intensity behavior at the pipe axis, where anisotropic effects are minimum, reveals that the turbulent intensity first decreases as the loading ratio is increased, but then increases. The mean gas velocity profile (not shown) and the fluctuating gas velocity profile significantly flatten with the addition of solids. The maximum in the mean gas velocity profile at the higher loadings even deviates from the tube centerline.

For the 500 μm particles, the turbulent intensity increases monotonically with increased loading at the pipe axis, although the turbulent energy is less than the clear gas intensity near the wall. Furthermore, at the highest solid loading investigated by Tsuji *et al.* (1984), the radial variation of the turbulent intensity is no longer monotonic, but it exhibits a minimum value at around $r/R = 0.6$. The effects on the mean gas velocity profile (not shown) observed with the 200 μm

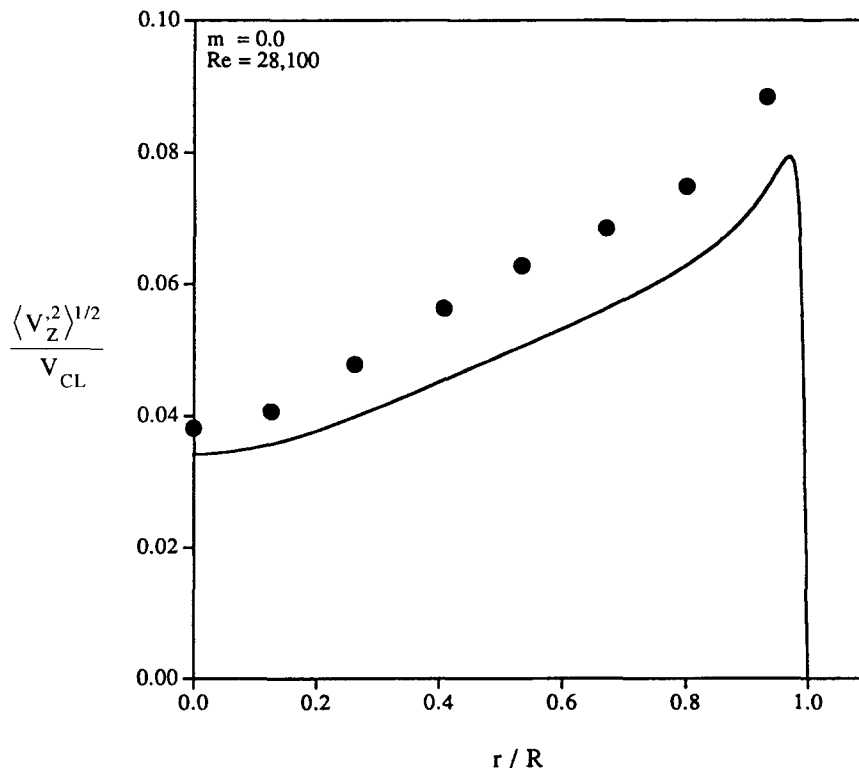


Figure 2. Radial variation of the r.m.s. axial fluctuating velocity component for a clear gas. The circles represent the experimental data of Tsuji *et al.* (1984).

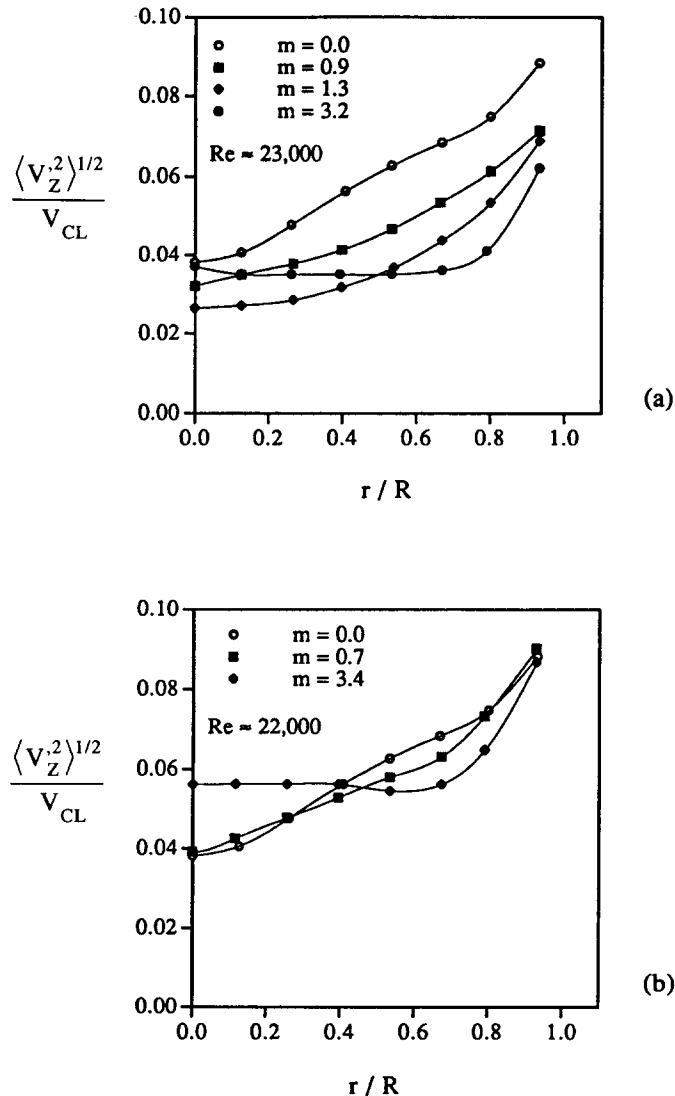


Figure 3. Experimental measurements of Tsuji *et al.* (1984) for the r.m.s. axial gas fluctuating velocity component at different solid loadings with (a) 200 μm and (b) 500 μm polystyrene spheres.

particles become more pronounced with increased particle size. The relative velocity increases with increasing particle size and decreases with solid loading.

RESULTS AND DISCUSSION

We first investigate the effect of changes in the mean gas velocity profile on the turbulent kinetic energy in the gas phase, neglecting any direct effect of the particle assembly on the gas phase turbulence by setting $\Delta K = 0$. Figure 4 illustrates that as the solid loading increases for a fixed Reynolds number, a progressive decrease in the r.m.s. axial gas velocity component is observed. This diminution in the gas velocity fluctuations is a result of the progressive flattening of the mean gas velocity profile and the corresponding decrease in the production of the turbulent kinetic energy. It should be noted that for smaller particles ($d < 50 \mu\text{m}$), a flattening of the mean velocity profiles has not been experimentally observed. Changes in the shape of the mean gas velocity profile with the larger particles can be attributed to changes in the mean solids velocity and solids volume fraction profile (Bolio *et al.* 1995). Hence, in the absence of any term describing gas turbulence modulation effects due to the addition of larger particles (ΔK), changes in the shape of the mean gas velocity profile alone results in a significant decrease in the magnitude of the gas phase

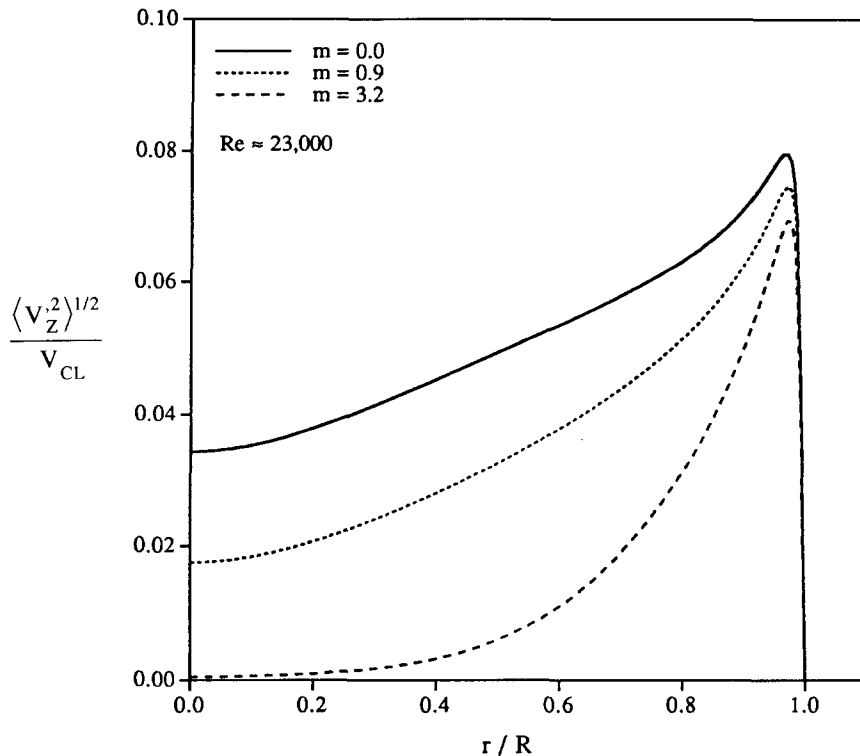


Figure 4. Model predictions when $\Delta K = 0$ for the radial variation of the r.m.s. axial gas fluctuating velocity component with $500 \mu\text{m}$ polystyrene spheres at three different solid loadings.

fluctuations. Thus, a mechanism for turbulence generation must be present in order to compensate for this effect; that is, the description for ΔK in the model must reflect a source of turbulence in order for the gas velocity fluctuations to be consistent with the measured values, even in the case where the experimental results indicate a net suppression of gas phase turbulence in the presence of particles.

Figure 5(a) and (b) presents predictions from the model which incorporates a source of gas turbulent fluctuations due to the presence of wakes (wake volume given by [9]) at operating conditions which coincide with the experimental observations of Tsuji reproduced in figure 3(a) and (b). The system parameters for all of the results to be presented are given in table 1. For the $200 \mu\text{m}$ particles [shown in figure 5(a)], the predicted profiles agree with the measurements in that they reveal gas turbulent intensities in the presence of particles less than the clear gas intensities throughout the pipe section, except for the region immediately adjacent to the wall, where a large peak in intensity is predicted. The presence of this peak is due to the large solid slip at the tube wall since the wake-related turbulent production is primarily dependent on the local relative velocity between the phases. These large slips at the wall were observed in the experimental measurements of Tsuji *et al.* (1984) and reproduced in our mean velocity predictions (Bolio *et al.* 1995). The presence of this peak cannot be confirmed by the experimental measurements because the peak occurs at a radial location closer to the wall than the closest measurement. The progressive

Table 1. Summary of system parameters

Particle diameter, d	200 μm , 500 μm
Particle density, ρ_s	1020 kg/m^3
Pipe radius, R	1.525 cm
Gas density, ρ_G	1.2 kg/m^3
Gas viscosity, μ	$1.75 \times 10^{-5} \text{ kg}/\text{m s}$
Coefficient of restitution for particle-particle collisions, e	0.94
Coefficient of restitution for particle-wall collisions, e_w	0.94
Specularity coefficient, ϕ	0.002
Solids volume fraction at closest packing, v_o	0.65

radial flattening of the turbulent intensity as the loading ratio is increased is also correctly reproduced by the predicted profiles. The flattening of the mean gas velocity profile with increased solid loading decreases the production of the turbulent kinetic energy and is responsible for the flattening observed in the fluctuating gas velocity profile. The model fails, however, to duplicate the increase in the centerline turbulent intensity at the highest solid loading. Instead, a progressive decrease in the centerline turbulent intensity is seen.

The predictions for the system of $500\ \mu\text{m}$ particles are shown in figure 5(b). At the pipe centerline, the turbulent intensity increases monotonically with increased solid loading. Close to the wall, but before the peak region, the turbulent intensity is lower than the clear gas intensity, as is shown in the data. For the highest solid loading $m = 3.4$, the turbulent intensity begins to decrease from the pipe centerline towards the wall. This effect was observed by Tsuji *et al.* (1984) at the same solid loading. As with the smaller particles, the peak predicted in the vicinity of the wall is due to the large particle slip at the wall. A distinctive feature of the predicted profiles, present at both loading ratios, is the presence of a small zone of turbulence suppression preceding the peak. The zone coincides with the crossover of the mean gas and particle velocity fields where the particle Reynolds number falls below ten and no wake effect is predicted. This zone is absent in the predictions for the $200\ \mu\text{m}$ particles since the relative importance of the wake-related turbulence production is less for the smaller particles.

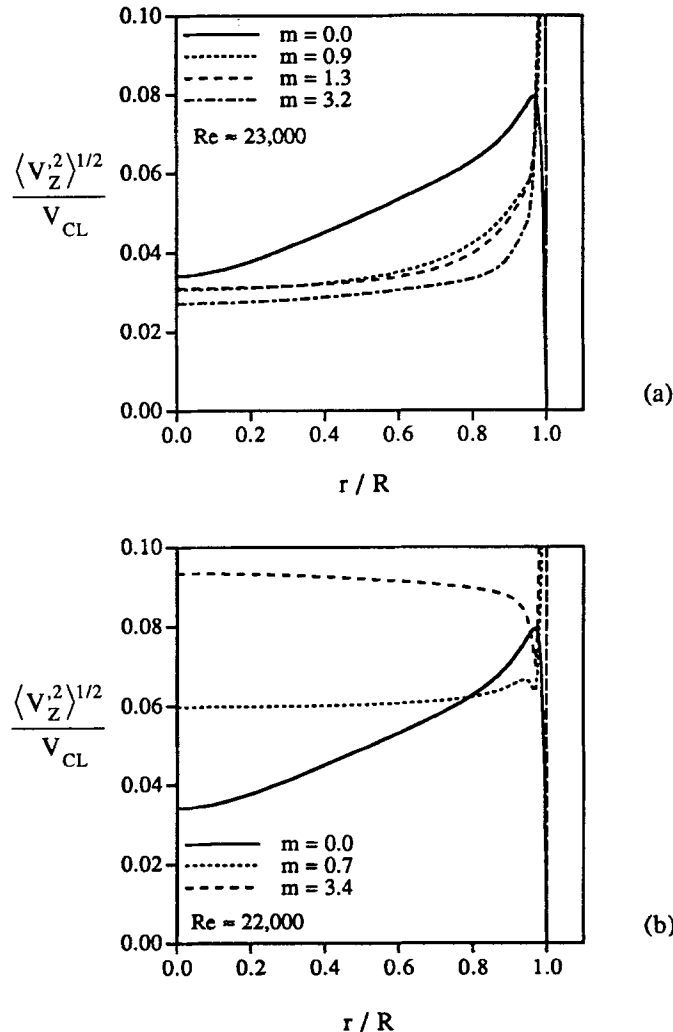


Figure 5. Model predictions for the radial variation of the r.m.s. axial gas fluctuating velocity component at different solid loadings for (a) $200\ \mu\text{m}$ and (b) $500\ \mu\text{m}$ polystyrene spheres.

Table 2. Predicted particle Reynolds numbers Re_p and particle diameter to eddy-length scale ratio for the 200 and 500 μm polystyrene spheres

Particle diameter, d	Solid loading, m	$Re_{p,CL}$	$Re_{p,max}$	$Re_{p,avg}$
200	0.9	30	138	12
200	1.3	27	139	12
200	3.2	16	121	11
500	0.7	120	294	72
500	3.4	97	263	71

Particle diameter, d	Solid loading, m	$d/l_{e,CL}$	$d/l_{e,avg}$	d/l_e^\dagger
200	0.9	0.09	0.20	0.07
200	1.3	0.08	0.20	0.07
200	3.2	0.08	0.20	0.07
500	0.7	0.15	0.33	0.16
500	3.4	0.13	0.26	0.16

† Estimated by Gore & Crowe (1989).

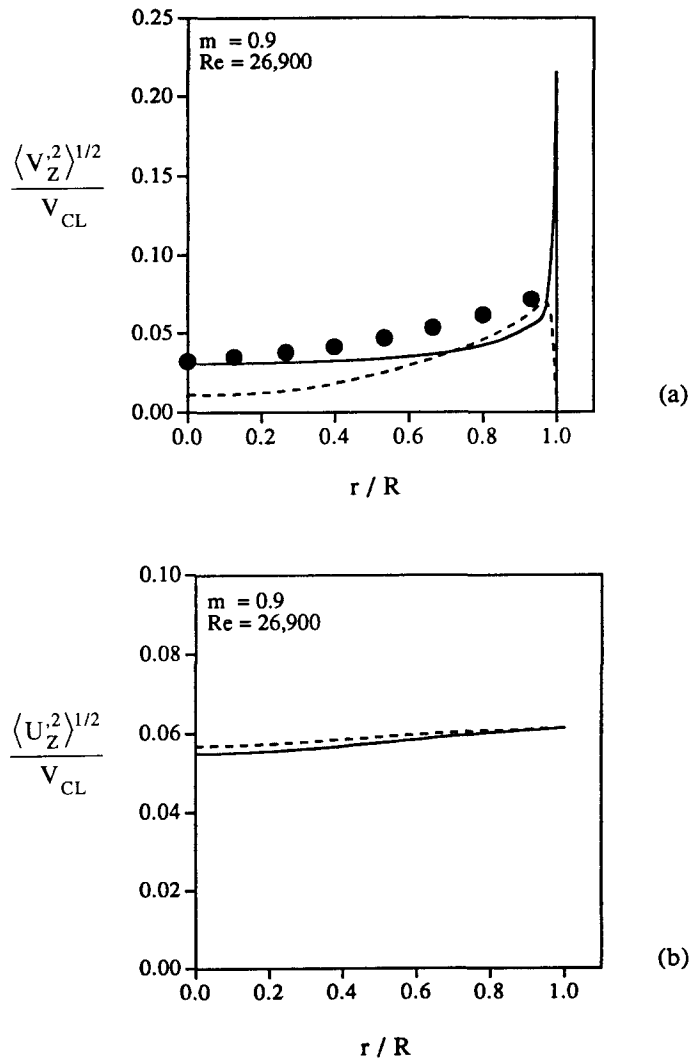


Figure 6. Radial variation of (a) r.m.s. gas velocity fluctuations and (b) r.m.s. solids velocity fluctuations with 200 μm polystyrene spheres at a solid loading of 0.9. The circles represent the data of Tsuji *et al.* (1984); - - - - - present model; — model given in Bolio *et al.* (1995).

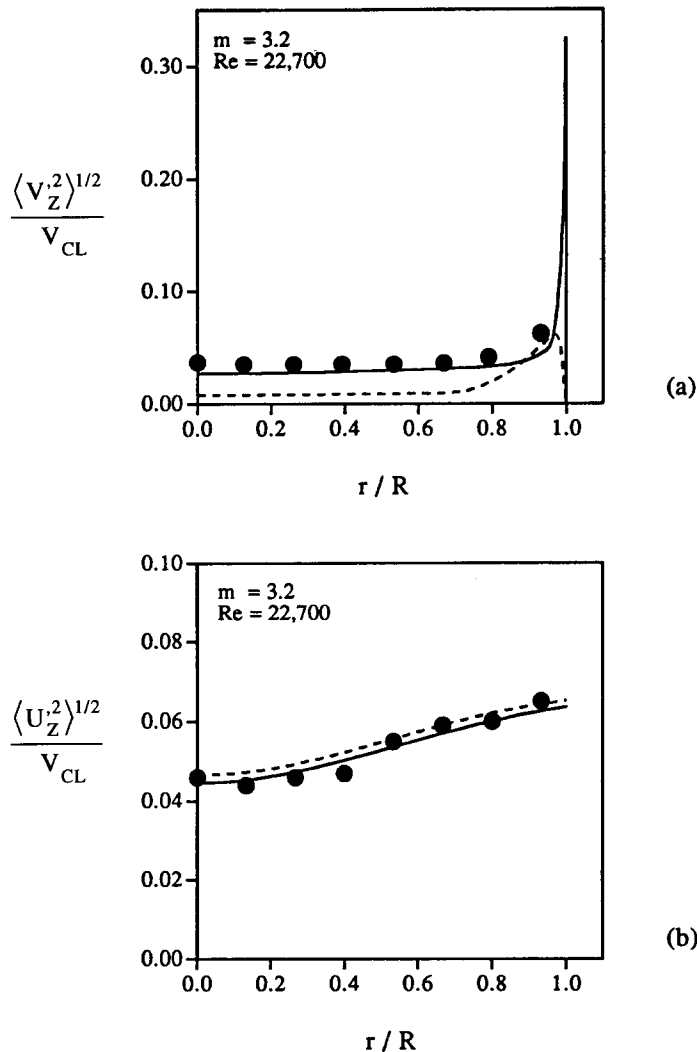


Figure 7. Radial variation of (a) r.m.s. gas velocity fluctuations and (b) r.m.s. solids velocity fluctuations with $200 \mu\text{m}$ polystyrene spheres at a solid loading of 3.2. The circles represent the data of Tsuji *et al.* (1984) and Tsuji (1993); - - - - - present model; — model given in Bolio *et al.* (1995).

An indication of the effect of the particle phase on the gas phase turbulence can be obtained by examining the particle Reynolds number Re_p , as suggested by Hetsroni (1989), or the ratio of the particle diameter to the most-energetic eddy length scale d/l_c as postulated by Gore & Crowe (1989). Table 2 compiles predicted values for the particle Reynolds number based on the present model. These Re_p values could alternatively have been generated directly from the experimental data for the relative velocity given by Tsuji *et al.* (1984). The differences, however, are small since the model predictions for the mean velocity were in good agreement with the experimental data (Bolio *et al.* 1995). At each operating condition, the particle Reynolds number ranges between zero, at the velocity crossover point, to a maximum value obtained at the wall where the relative velocity is the largest. Table 2 also includes the centerline (CL) and radially-averaged values for Re_p .

Achenbach (1974) showed that vortex shedding occurred for flows with $Re_p > 400$. None of the conditions investigated by Tsuji *et al.* (1984) with the 200 and $500 \mu\text{m}$ particles exceed this Re_p . Hence, most likely, the wake effect, rather than vortex shedding, is contributing to turbulence generation for these conditions. In addition, since the Re_p for all of these flows is less than 400, turbulent intensities exceeding the single phase values are only observed near the pipe axis for the $500 \mu\text{m}$ particles and not throughout the domain. It may be that Hetsroni's criterion will

correspond to an increase in turbulent intensity for two phase flow over single phase flow throughout the domain when the Re_p exceeds 400.

The d/l_c criterion devised by Gore & Crowe (1989) provides an estimate of whether the relative turbulent intensity of the gas phase will increase or decrease by the addition of the particles. For the $200\ \mu\text{m}$ particles, using the l_c generated by the model (which is dependent on the solid loading, Reynolds number and varies with radial position) and the estimate given by Gore & Crowe ($l_c = 0.2R$ for the entire cross-section), the d/l_c ratio in all cases is slightly under the critical value of 0.1 at the centerline. Hence, the Gore & Crowe criterion would estimate a gas turbulent intensity in the presence of particles lower than the corresponding single phase intensity. For the lowest solid loading this criterion is consistent with the data although this criterion does not seem to capture the fact that the turbulent intensity at the centerline for two phase flows equals that for single phase flow at the highest solid loading. In addition, for the $200\ \mu\text{m}$ particles, the average d/l_c ratio exceeds the critical value for all solid loadings although the experimental observation indicates a relative suppression of turbulence (except at the pipe centerline with the highest solid loadings, as just discussed). For the $500\ \mu\text{m}$ particles, the centerline and average ratio are consistent with the criterion developed by Gore & Crowe (1989) for the centerline turbulent intensity. The

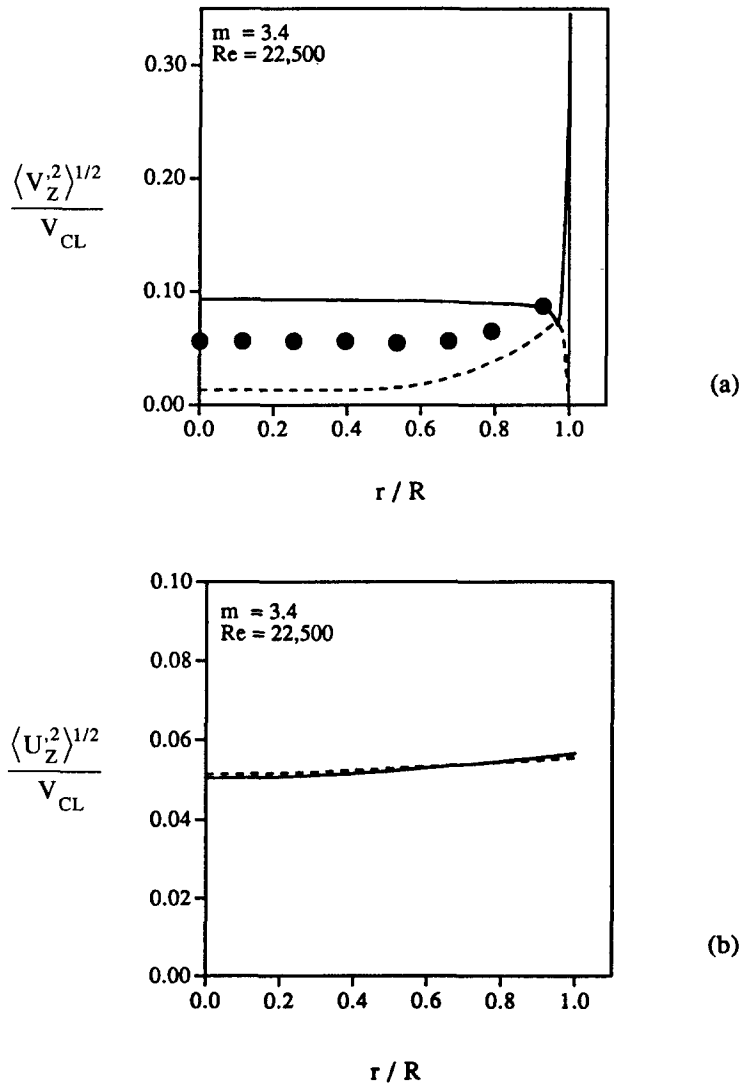


Figure 8. Radial variation of (a) r.m.s. gas velocity fluctuations and (b) r.m.s. solids velocity fluctuations with $500\ \mu\text{m}$ polystyrene spheres at a solid loading of 3.4. The circles represent the data of Tsuji *et al.* (1984); - - - - - present model; — model given in Bolio *et al.* (1995).

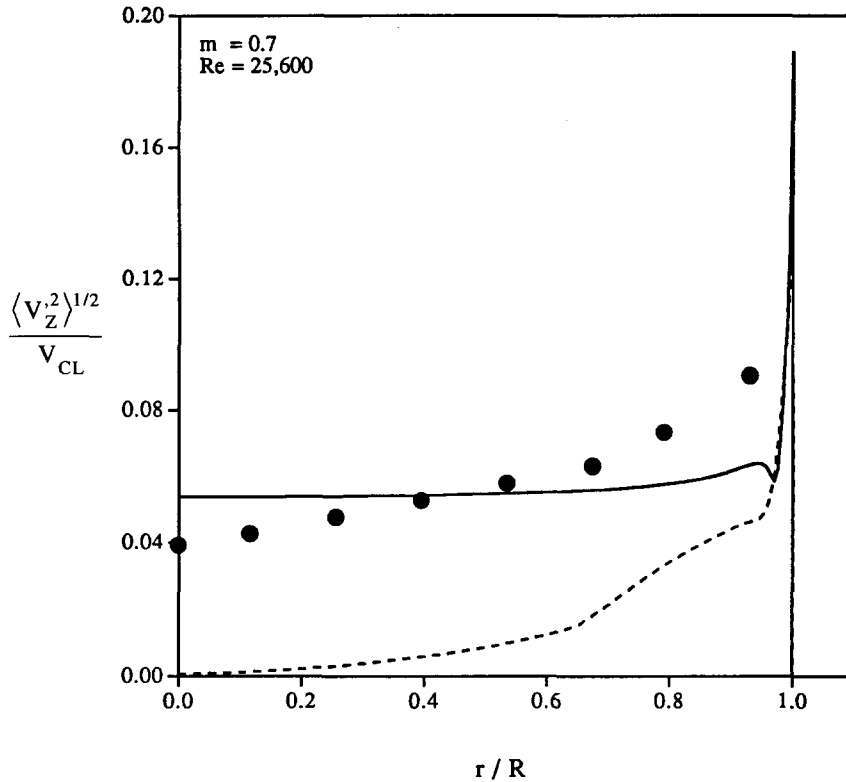


Figure 9. Radial variation of r.m.s. axial gas fluctuating velocity for 500 μm polystyrene spheres. The circles represent the data of Tsuji *et al.* (1984); - - - - - present model; — predictions from a model which incorporates turbulence damping and production following the treatment of Yuan & Michaelides (1992).

turbulent intensity near the wall at both solid loadings, however, is still less than the single phase intensity.

Figures 6, 7 and 8 depict predictions for the gas and particle velocity fluctuations and comparisons with the experimental data of Tsuji *et al.* (1984) and Tsuji (1993) when available. The solid lines represent the predictions from the present model which includes a mechanism for turbulence generation due to the presence of wakes while the dashed line represents predictions from a model in which gas turbulence modulation is described following the treatment of Louge *et al.* (1991) and Bolio *et al.* (1995). For the 200 μm particles (figures 6 and 7) the centerline intensity is captured well by the current model. For all of the operating conditions investigated, the particle fluctuation intensity predictions are only slightly altered by the change in our closure for ΔK and are in excellent agreement with the data. With the 500 μm particles (figure 8), the centerline intensity is overestimated by the current closure for ΔK , most notably so at the highest solid loading investigated by Tsuji *et al.* (1984). The lack of a mechanism for turbulent dissipation may be responsible for this discrepancy.

In an attempt to include such a dissipation mechanism, the treatment of Yuan & Michaelides (1992) is once again employed. Yuan & Michaelides (1992) postulate a description for the dissipation of turbulent kinetic energy by the particles by analyzing the rate of work done by the fluid to drag the particle (equation 3 in their paper). In figure 9 the solid line indicates the predictions from a model which includes turbulence generation only; the dashed line indicates predictions from a model which includes turbulence generation and dissipation. The figure represents the results with 500 μm spheres at the lowest solid loading investigated by Tsuji *et al.* (1984). The predicted turbulence damping is unrealistically large and dominates the generation term even though the particle relaxation time is much larger than the particle-eddy interaction time. It should be noted that in the study of Yuan & Michaelides (1992) the authors include an assessment of their proposal for the overall gas turbulence modulation (enhancement and dissipation) by

comparing with the experimental data of Tsuji *et al.* (1984), and they showed good agreement with the data. However, in order to perform this evaluation, assumed profiles for the gas and solid velocities were required. The gas velocity profile was assumed to follow the single phase, 1/7th velocity profile form. The particle velocity profile was assumed to follow the gas velocity profile with a constant relative velocity equal to the particle terminal velocity. However, as discussed previously, the magnitude of the relative velocity varies significantly over the tube cross-section. In fact, the magnitude of the relative velocity can vary from zero at the crossover point up to a factor of ten times the particle terminal velocity. The gas velocity profiles also deviate significantly from their shape in single phase flow. These assumptions cast doubt on the conclusions derived from the assessment. Nevertheless, one could still explain the discrepancy in figure 9 as due to the lack of an adequate description for a dissipative mechanism, as well as many other factors. One explanation could be that the present description for gas turbulence modulation neglects the effect on each particle wake when particles interact or come in close contact. This effect would become more significant as the suspension becomes more concentrated.

Representative results from the present model, including the improved estimate of the wake volume, are included in figure 10. The solid line indicates the predictions from the present model

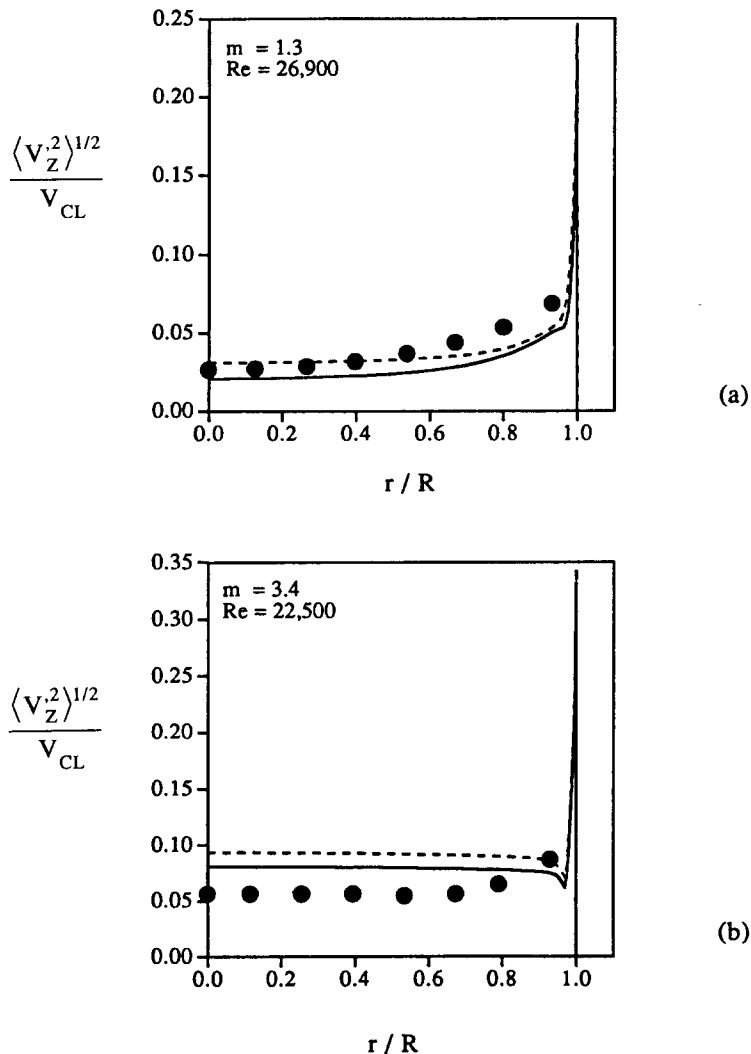


Figure 10. Radial variation of r.m.s. axial gas velocity fluctuations for (a) 200 μm and (b) 500 μm polystyrene spheres. The circles represent the data of Tsuji *et al.* (1984); - - - - - model predictions incorporating a wake volume given by [10] and [11]; — model predictions incorporating a wake volume given by [9].

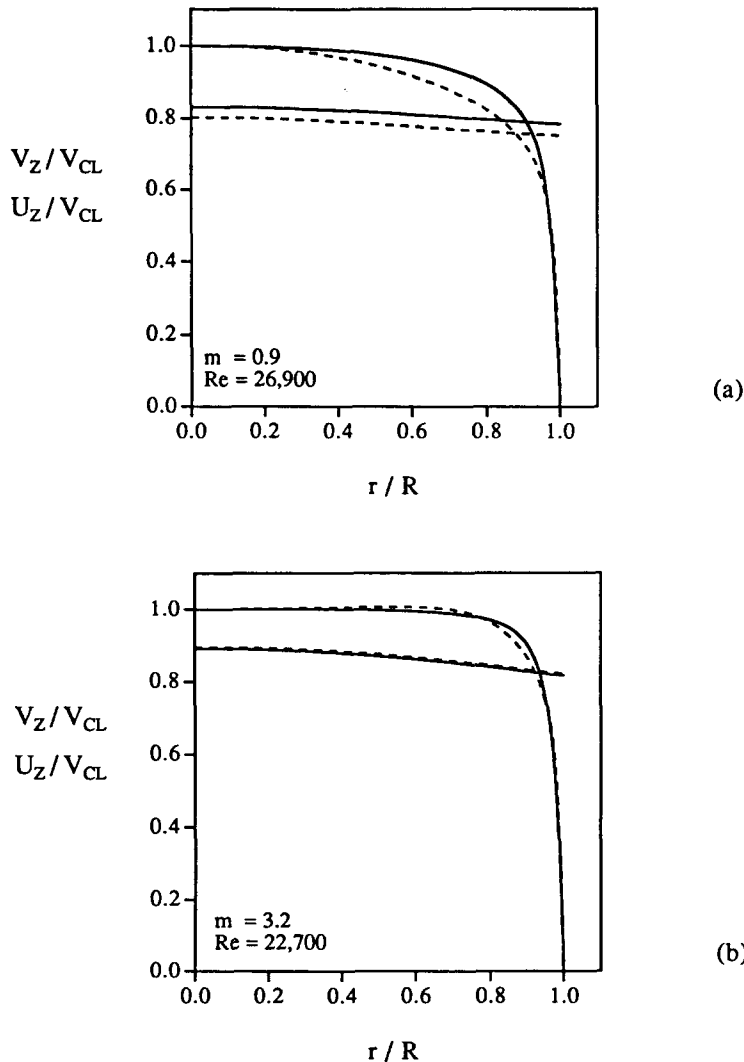


Figure 11. Predictions for the radial variation of mean gas and solids velocity for 200 μm polystyrene spheres at two different loadings: - - - - - present model; — model given in Bolio *et al.* (1995).

incorporating a wake volume given by [10] and [11] rather than [9] which was used to generate the previous figures. The improved estimate results in a slight reduction of the wake volume, and the magnitude of the turbulence generation due to the presence of wakes is diminished.

Figure 11 presents the mean velocity profiles at the same operating conditions shown in figures 6 and 7. The solid line presents the results of the current model which includes a mechanism for turbulence generation due to particle wakes; the dashed line indicates the predictions from the previous model in which turbulence modulation is described following the treatment of Louge *et al.* (1991) and Bolio *et al.* (1995). The mean velocity profiles are only slightly altered at the lowest loadings for the 200 and 500 μm particles (not shown) with the change in the description for the gas turbulence modulation. In all of the cases investigated, the gas velocity profile slightly flattens and the relative velocity is slightly reduced. In general, the mean gas velocity profile was not significantly affected by the description for the gas turbulence modulation, but rather by the particle phase motion and concentration.

CONCLUSIONS

The presence of wakes behind particles is an important mechanism in gas turbulence modulation. This is true even in the case when the net gas turbulent intensity for two phase flow is less than

the corresponding single phase flow intensity due to the significant flattening of the mean gas velocity profile upon the addition of larger particles and the resulting decrease in the production of turbulent kinetic energy. The proposed model, which accounts for particle–particle interactions associated with larger particles, describes the process of turbulent enhancement accounting for the effect of wakes following a proposal by Yuan & Michaelides (1992). Fairly good qualitative and quantitative agreement between the theoretical and experimental results of Tsuji *et al.* (1984) is achieved. The treatment of Yuan & Michaelides, albeit simple, appears to have identified key variables influencing gas turbulence enhancement in dilute phase flow with larger particles.

Acknowledgements—The authors gratefully acknowledge funding support from the National Science Foundation Presidential Young Investigator Awards Program Grant No. CTS-9157185 and the Dow Chemical Company. The authors would also like to thank Professor Tsuji for providing the experimental measurements of the solid velocity fluctuations.

REFERENCES

- Achenbach, E. 1974 Vortex shedding from spheres. *J. Fluid Mech.* **62**, 565–575.
- Bolio, E., Yasuna, J. & Sinclair, J. 1995 Dilute turbulent gas–solid flow in risers with particle–particle interactions. *AIChE JI* **41**, 1375–1388.
- Ding, J. & Gidaspow, D. 1990 A bubbling fluidization model using kinetic theory analogy of granular flow. *AIChE JI* **36**, 523–538.
- Gore, R. & Crowe, C. 1989. Effect of particle size on modulating turbulent intensity. *Int. J. Multiphase Flow* **15**, 279–285.
- Hetsroni, G. 1989 Particles–turbulence interaction. *Int. J. Multiphase Flow* **15**, 735–746.
- Hrenya, C., Bolio, E., Chakrabarti, D. & Sinclair, J. 1995 Comparative study of low Reynolds $k-\epsilon$ models in predicting turbulent pipe flow. *Chem. Engng Sci.* **50**, 1923–1941.
- Johnson, P. & Jackson R. 1987 Frictional–collisional constitutive relations for granular materials, with application to plane shearing. *J. Fluid Mech.* **176**, 67–93.
- Koch, D. 1990 Kinetic theory for a monodisperse gas–solid suspension. *Phys. Fluids A* **2**, 1711–1723.
- Lee, S. & Durst, F. 1982 On the motion of particles in turbulent duct flows. *Int. J. Multiphase Flow* **8**, 125–146.
- Louge, M., Mastorakos, E. & Jenkins, F. 1991 The role of particle collisions in pneumatic transport. *J. Fluid Mech.* **231**, 345–359.
- Lun, C., Savage, S., Jeffrey, D. & Chepurnyi, N. 1984 Kinetic theories for granular flows; inelastic particles in couette flow and slightly inelastic particles in a general flow field. *J. Fluid Mech.* **140**, 223–256.
- Maeda, M., Hishida, K. & Furutani, T. 1980 Optical measurements of local gas and particle velocity in an upward flowing dilute gas–solids suspension. *Polyphase Flow and Transport Technology*, Century 2-ETC, pp. 211–216.
- Martinuzzi, R. & Pollard, A. 1989 Comparative study of turbulence models in predicting turbulent pipe flow. *AIAA JI* **27**, 29–36.
- Myong, H. & Kasagi, N. 1990 A new approach to the improvement of $k-\epsilon$ turbulence model for wall-bounded shear flows. *JSME Int. J. Series II* **33**, 63–72.
- Ocone, R., Sundaresan, S. & Jackson, R. 1993 Gas–particle flow in a duct of arbitrary inclination with particle–particle interactions. *AIChE JI* **39**, 1261–1271.
- Pita, J. & Sundaresan, S. 1993 Developing flow of a gas–particle mixture in a vertical riser. *AIChE JI* **39**, 541–552.
- Rimon, Y. & Cheng, S. 1969 Numerical solution of a uniform flow over a sphere at intermediate Reynolds numbers. *Phys. Fluids* **12**, 949–959.
- Schildknecht, M., Miller, J. & Meier, G. 1979 The influence of suction on the structure of turbulence in fully-developed pipe flow. *J. Fluid Mech.* **90**, 67–107.
- Sinclair, J. & Jackson, R. 1989 Gas–particle flow in a vertical pipe with particle–particle interactions. *AIChE JI* **35**, 1473–1486.

Tsuji, Y. 1993 Private communication.

Tsuji, Y., Morikawa, Y. & Shiomi, H. 1984 LDV measurements of an air–solid two-phase flow in a vertical pipe. *J. Fluid Mech.* **139**, 417–434.

Yuan, Z. & Michaelides, E. 1992 Turbulence modulation in particulate flows—a theoretical approach. *Int. J. Multiphase Flow* **18**, 779–785.